Carbohydrate Research 531 (2023) 108896

Contents lists available at ScienceDirect

Carbohydrate Research

journal homepage: www.elsevier.com/locate/carres

Immunochemical studies and gene cluster relationships of closely related O-antigens of *Aeromonas hydrophila* Pt679, *Aeromonas popoffii* A4, and *Aeromonas sobria* K928 strains classified into the PGO1 serogroup dominant in Polish aquaculture of carp and rainbow trout

Maria Kurzylewska [a], Anna Turska-Szewczuk [a,*], Katarzyna Dworaczek [a], Arkadiusz Bomba [b], Dominika Drzewiecka [c], Agnieszka Pękala-Safińska [d]

[a] *Department of Genetics and Microbiology, Institute of Biological Sciences, M. Curie-Sklodowska University, Akademicka 19, 20-033, Lublin, Poland*
[b] *Department of Omics Analyses, National Veterinary Research Institute, Partyzantow 57, 24-100, Pulawy, Poland*
[c] *Laboratory of General Microbiology, Department of Biology of Bacteria, Faculty of Biology and Environmental Protection, University of Lodz, Banacha 12/16, 90-237, Lodz, Poland*
[d] *Department of Preclinical Sciences and Infectious Diseases, Faculty of Veterinary Medicine and Animal Science, Poznan University of Life Sciences, Wolynska 35, 60-637, Poznan, Poland*

ARTICLE INFO

Keywords:
Aeromonas
O-antigen
O-antigen gene cluster
QuiNAc
Fuc*p*3NAc
NMR

ABSTRACT

The present study included three *Aeromonas* sp. strains isolated from fish tissues during Motile Aeromonas Infection/Motile Aeromonas Septicaemia disease outbreaks on commercial farms, i.e.: *Aeromonas hydrophila* Pt679 obtained from rainbow trout as well as *Aeromonas popoffii* A4 (formerly *Aeromonas encheleia*) and *Aeromonas sobria* K928 both isolated from carp, which were classified into the new provisional PGO1 serogroup prevailing among aeromonads in Polish aquaculture. The structure of the O-specific polysaccharides of A4 and K928 has been previously established. Here, immunochemical studies of the O-specific polysaccharide of *A. hydrophila* Pt679 were undertaken. The O-specific polysaccharide was obtained from the lipopolysaccharide of *A. hydrophila* Pt679 after mild acid hydrolysis and separation by gel-permeation chromatography. The high-molecular-mass fraction was studied using chemical methods and ^{1}H and ^{13}C NMR spectroscopy, including ^{1}H,^{1}H NOESY, and ^{1}H,^{13}C HMBC experiments. The following structure of the branched repeating unit of the O-polysaccharide from *A. hydrophila* Pt679 was determined:

→3)[α-D-Fuc*p*3NAc-(1→2)]-α-L-Rha*p*-(1→3)-β-L-Rha*p*-(1→4)-α-L-Rha*p*-(1→3)-β-D-Qui*p*NAc-(1→2)┘

The studies indicated that O-polysaccharides from *A. hydrophila* Pt679, *A. popoffii* A4 and *A. sobria* K928 share similarities but they also contain unique characteristics. Western blotting and an enzyme-linked immunosorbent assay revealed that the cross-reactivity of the related O-antigens is caused by the occurrence of common structural elements, whereas additional epitopes define the specificity of the O-serotypes.

For genetic relationship studies, the O-antigen gene cluster was characterized in the genome of the *A. hydrophila* Pt679 strain and compared with the corresponding sequences of *A. popoffii* A4 and *A. sobria* K928 and with sequences available in the databases. The composition of the regions was found to be consistent with the O-antigen structures of *Aeromonas* strains classified into the same PGO1 serogroup.

* Corresponding author.
E-mail address: anna.turska-szewczuk@mail.umcs.pl (A. Turska-Szewczuk).

https://doi.org/10.1016/j.carres.2023.108896
Received 19 May 2023; Received in revised form 3 July 2023; Accepted 5 July 2023
Available online 7 July 2023
0008-6215/© 2023 The Authors. Published by Elsevier Ltd. This is an open access article under the CC BY license (http://creativecommons.org/licenses/by/4.0/).

1. Introduction

The genus *Aeromonas* sp. comprises Gram-negative bacilli-shaped bacteria positive for catalase and oxidase tests, glucose fermentation and nitrate degradation, which are commonly found in aquatic environments [1]. They include psychrophilic (temperature range of 22–25 °C) and mesophilic (optimal growth at 35–37 °C) representatives, both being responsible for infections in various fish species, whereas the latter ones are frequently recognized as important causative agents of human diseases. In fish, Motile Aeromonad Infection and Motile Aeromonad Septicaemia (MAI/MAS) diseases pose the greatest threat [2], as they lead to mass fish deaths and thus large economic losses in aquacultures around the world. In Poland, the diseases affect the population of carp (*Cyprinus carpio*) and rainbow trout (*Oncorhynchus mykiss*), which are the main cultured fish species [3,4].

Aeromonas spp. are equipped with many virulence factors, which allow them to attach, colonize and then damage host's cells [5]. Among them, the most important agent promoting the pathogenicity of Gram-negative bacteria is lipopolysaccharide (LPS). LPS is a surface glycoconjugate anchored in the outer membrane and mutations affecting its synthesis may contribute to loss of virulence. LPS typically consists of three moieties: the hydrophobic lipid A (being the centre of endotoxin activity), nonrepeating "core" oligosaccharide (OS), and O-specific polysaccharide (OPS) or O-antigen [6,7]. Due to its association with bacterial virulence, lipopolysaccharide is one of the pathogen-associated molecular patterns (PAMPs) and is a ligand recognized by the pathogen recognition receptor (PRR) of the immune system effector cells. The PRRs include toll-like receptors (TLRs), which are the main signalling cofactors of pathogen invasion. The TLR-family includes TLR-4, which participates in LPS recognition and is present in mammals, while in fish it is found only in *Danio rerio* and cyprinids [8,9].

The O-antigen is the most external part of the LPS molecule and consists of polysaccharides with hypervariable repeating units that may be linear or branched [6,7]. The current interest in the O-polysaccharide structure and genetics results from its basic role, i.e. the protective function against innate immunity defence as well as the possibility of potential application in vaccine development. The structure of the O-antigen defines the serological specificity of bacteria, and modifications in O-repeat units create new, provisional serogroups [6]. In *Aeromonas*, almost one hundred serogroups have been described. However, due to the high antigenic variability among strains, new provisional serogroups should be added here, but their number of still remains undetermined [1]. In Poland, virulent *Aeromonas* are mainly identified within the classical NIH system (O3, O6, O11, O16, O18, O33, O34) and provisional serogroups (PGO1, PGO2, PGO4, PGO6) [2].

The high diversity in the structure of the O-antigen is related to the genetic variability of the O-antigen gene cluster (OGC), essential for its biosynthesis, and switching within the O-serotype results from alterations in the sets of the OGC genes. The organization of clusters has been well-studied in several representatives of the Enterobacteriaceae family, but is only partially known in *Aeromonas*. The OGC comprises genes involved in the biosynthesis of activated sugars, glycosyltransferases, and O-antigen polymerases, as well as enzymes crucial for the export of the final O-unit product on the cytoplasmic surface of the inner membrane, where polymerization occurs. So far, only three O-antigen biosynthesis pathways have been recognized: the Wzx/Wzy-dependent pathway, the ABC transporter-dependent pathway, and the synthase-dependent pathway. Flippase (Wzx), O-antigen polymerase (Wzy), O-antigen ligase (WaaL), and O-antigen length determinator (Wzz) are proteins involved in the Wzx/Wzy-pathway [7,10,11]. In this type, the individual O-repeating units are assembled at the cytoplasmic face of the inner membrane and then transported by Wzx. Polymerization of O-units by Wzy polymerase occurs in the periplasmic face of the inner membrane [11,12]. In the pathway which depends on the ABC-transporter, the elongation of the O-antigen by glycosyltransferases takes place entirely on the cytoplasmic surface of the inner membrane. The synthase-dependent secretion system has only been described for the plasmid-encoded *S. enterica* O54 O-antigen, which is a homopolymer of N-acetylmannosamine [13].

Elucidation of the structure and genetics of the O-antigen assembly will contribute to the classification of bacteria for better detection and rapid serotyping, and thus may improve strategies to prevent and control *Aeromonas* sp. infections.

The present paper reports on the immunochemistry of the *A. hydrophila* Pt679 O-antigen and the genetic basis of its synthesis. In addition, a comparison of the structure of Pt679 and two related O-antigens of *A. popoffii* A4 and *A. sobria* K928 [14,15] classified into the same PGO1 serogroup, and the genetic organization of their OGC regions was also performed.

Western blotting and ELISA experiments facilitated identification of common structural elements within the related O-antigens and recognition of epitopes that define their specificity. The representatives of the PGO1 serogroup and the dominant immunotype among *Aeromonas* spp. pathogenic to fish in Polish aquaculture are the first three strains whose O-serotypes have been completely recognized genetically and structurally.

2. Experimental

2.1. Bacterial strain and growth conditions

A. hydrophila Pt679 was isolated from rainbow trout kidney during an outbreak of MAI/MAS disease on a Polish fish farm, and classified into the provisional O-serogroup PGO1 after agglutination assays with antisera of the NIH scheme [16] and 20 additional antisera developed for Polish isolates representing new provisional serogroups (PGO1—PGO20) [2,17].

For the LPS isolation, *A. hydrophila* strain Pt679 was cultivated with aeration at 28 °C in a tryptic soy broth (TSB) medium. After 3 days, the cells were harvested by centrifugation (8000×*g*, 35 min).

2.2. Extraction of LPS

LPS was extracted from the cell biomass of *A. hydrophila* strain Pt679 with the classical hot phenol/water method [18] followed by separation of the water and phenol layers by low speed centrifugation (3000×*g*, 1 h). After extensive dialyses against tap water and, after the smell of phenol disappeared with distilled water, LPS species were recovered through ultracentrifugation (105,000×*g*, 3 h) and freeze-drying. The high molecular-weight S-LPS species were found in the phenol phase in the yield ~2% of dry cell biomass.

2.3. SDS-PAGE analysis

The phenol-soluble LPS samples of *A. hydrophila* Pt679 and two other *Aeromonas* strains i.e., *A. popoffii* A4 and *A. sobria* K928, were prepared in sample buffer (2% SDS and 50 mM Tris/HCl (pH 6.8), 25% glycerol, 0.1% bromophenol blue) and then separated in 12.5% SDS-Tricine polyacrylamide electrophoresis gel. The profiles were visualized by staining with silver nitrate after oxidation with periodate according to the published method [19].

2.4. Serological studies (Western blotting and ELISA)

Polyclonal O-antisera against *A. hydrophila* Pt679, *A. popoffii* A4 and *A. sobria* K928 were obtained by immunization of New Zealand white rabbits with three doses of bacteria (0.25, 0.5, and 1.0 ml) inactivated by 2.5-h boiling. Eight days after the last injection, 18-day antisera were obtained, according to the published method [20]. All the experiments were performed according to the procedures approved by the local ethical committee (The Ninth Local Ethical Committee on Animal Testing in Lodz, permission number 51/ŁB 218/2021). The polyclonal

rabbit O-antiserum against the *Aeromonas* sp. reference strain for the provisional serogroup PGO1 was a kind gift from Professor Alicja Kozińska (the National Veterinary Research Institute, Puławy, Poland) [17].

Western blotting experiments with rabbit antisera were performed after transferring SDS-PAGE-separated LPS samples of *A. hydrophila* Pt679, *A. popoffii* A4, and *A. sobria* K928 onto Immobilon P (Millipore, St. Louis, MO, USA). The primary antibodies were detected using alkaline phosphatase-conjugated goat anti-rabbit antibodies (Sigma, St. Louis, MO, USA). The blot was developed with nitroblue tetrazolium and 5-bromo-4-chloro-3-indolylphosphate toluidine (Sigma) for 5 min as described elsewhere [21].

The enzyme-linked immunosorbent assay (ELISA) was performed as described previously [20] with some modifications. In short: 0.1 μg of the *A. hydrophila* Pt679, *A. popoffii* A4, or *A. sobria* K928 LPS per well were coated on flat-bottom Nunc-Immuno plates; polyclonal rabbit reference PGO1 antiserum and O-antisera against *A. hydrophila* Pt679, *A. popoffii* A4, and *A. sobria* K928 as well as rabbit-IgG specific peroxidase-conjugated goat antibodies (Jackson ImmunoResearch, West Grove, PA, USA) were used. 2,2′-Azino-bis(3-ethylbenzothiazoline-6-sulfonic acid) diammonium salt (ABTS) (Sigma-Aldrich, USA) was used as a substrate for peroxidase; the absorbance (A_{405}) was measured with the help of a Multiskan Go microplate reader (Thermo Fisher Scientific Vantaa, Finland). The polyclonal antisera diluted 1:100 in PBS (phosphate-buffered saline) were three times adsorbed on Pt679, A4, or K928 cells during 0.5 h incubation on ice, in the ratio of 100 μl of wet biomass to 1 mL of the diluted serum. Then, the cells were removed by centrifugation [22].

2.5. Isolation of the Pt679 O-polysaccharide

An LPS sample (120 mg) of *A. hydrophila* Pt679 was subjected to hydrolysis with aq 2% acetic acid at 100 °C for 3 h and the lipid A precipitate was removed by centrifugation (13,000×*g*, 30 min). The O-polysaccharide fraction was obtained by fractionation of the supernatant containing the carbohydrate material by gel-permeation chromatography (GPC) on a Sephadex G-50 fine column (1.8 × 80 cm) in 1% acetic acid and monitored with a differential refractometer (Knauer, Germany). The OPS was obtained in a yield 14% of the LPS mass subjected to hydrolysis.

2.6. Chemical analyses

For sugar analysis, an OPS sample of *A. hydrophila* Pt679 was hydrolyzed with 2 M CF_3CO_2H (100 °C, 4 h), reduced with $NaBD_4$, and peracetylated with a 1:1 (v/v) Ac_2O-pyridine mixture (85 °C, 0.5 h). Monosaccharides were identified by GLC-MS of alditol acetates on an Agilent Technologies 7890A gas chromatograph (USA) connected to a 5975C MSD detector (inert XL EI/CI, Agilent Technologies, USA). The chromatograph was equipped with an HP-5MS capillary column (Agilent Technologies, 30 m × 0.25 mm, flow rate of 1 ml min^{-1}, He as the carrier gas). The temperature program was as follows: 150 °C for 5 min, then 150–310 °C at 5 °C min^{-1}, and the final temperature was maintained for 10 min.

Methylation of the OPS (1.5 mg) was performed with CH_3I in dimethyl sulfoxide in the presence of sodium hydroxide as described elsewhere [23]. The partially methylated alditol and aminoalditol acetates (PMAA) obtained after hydrolysis with 2 M CF_3CO_2H at 120 °C for 2 h, *N*-acetylation, reduction with $NaBD_4$, and peracetylation were analysed by GLC-MS.

The absolute configuration of Rha and QuiN was determined by GLC of acetylated (*S*)-(+)-2-octyl- and racemic 2-octyl-glycoside derivatives using authentic sugar standards as described previously [24]. The absolute configuration of Fuc3N was determined based on the analysis of glycosylation effects on ^{13}C resonances in the studied O-polysaccharide.

2.7. NMR spectroscopy

For structural assignments, 1D and 2D NMR spectra for an OPS sample (6 mg) were recorded in 99.98% D_2O at 32 °C on a 500 MHz NMR Varian Unity Inova instrument and calibrated with external acetone (δ_H 2.225, δ_C 31.45). Standard Varian software (Vnmrj V. 4.2 rev.) was used to acquire and process the NMR data. Homonuclear and heteronuclear two-dimensional experiments: $^1H,^1H$ TOCSY, $^1H,^1H$ DQF-COSY, $^1H,^1H$ NOESY, $^1H,^{13}C$ HSQC, and $^1H,^{13}C$ HMBC were carried out for signal assignments and determination of the sugar sequence. The mixing time of 100 and 200 ms was used in the TOCSY and NOESY experiments, respectively. The $^1H,^{13}C$ HSQC spectrum (band-selective gHSQCAD) measured without ^{13}C decoupling was used to determine the $^1J_{C1,H1}$ coupling constants for the anomeric carbons. The heteronuclear multiple-bond correlation ($^1H,^{13}C$ HMBC) experiment was optimized for $J_{C,H} = 8$ Hz, with 2-step low-pass filter 130 and 165 Hz to suppress one-bond correlations.

2.8. DNA isolation, whole genome sequencing, and bioinformatics analyses of OGCs

Genomic DNA of the *A. hydrophila* Pt679 and *A. popoffii* A4 strains were isolated using the bacterial DNA Extraction Kit (EuriX, Poland) according to the manufacturer's protocol and measured with Quant-iT PicoGreen dsDNA (Life Technologies). For sequencing library construction, genomic DNA of Pt679 and A4 were sheared on an ultrasonicator (Covaris E210) and prepared by the NEBNext® Ultra™ II DNA Library Prep Kit for Illumina (New England Biolabs). Sequencing was performed on a MiSeq instrument (Illumina, USA) using the v3 (2 × 300 bp) reagent kit. Raw reads after adapter trimming (fastp 0.12.4 [25]) and quality control (FastQC 0.11.9 [26]) yielded 534,057 Mbp and 512, 931 Mbp for *A. hydrophila* Pt679 and *A. popoffii* A4, respectively. The draft genomes were assembled using SPAdes 3.15.3 [27]. The quality of the assembly was evaluated using QUAST 5.0.2 [28]. The genomes were annotated using prokka 1.14.5 [29] with TIGRFAMs, Pfam-A, and HAMAP databases. A set of *A. hydrophila* and *A. sobria* K928 O-antigen gene cluster sequences deposited in GenBank with accession numbers MH449673-MH449686 [30] and OQ411005 [15], respectively, was used to determine the prokka '–proteins' option.

The O-antigen gene cluster sequences of *A. hydrophila* Pt679 and *A. popoffii* A4 strains were deposited in GenBank under the Accession Numbers: OQ984065 and OQ984064, respectively. Visualization of the Pt679 and A4 OGCs was generated by Clinker 0.0.26 [31].

For species identification, the 16S rRNA gene of Pt679 was BLAST-ed (blastn 2.12.0) to the SILVA 138 SSU database. Moreover, MLPA (multilocus phylogenetic typing analysis) of Pt679 and A4 isolates was done based on *gyrB*, *rpoD*, *recA*, *dnaJ*, *gyrA*, *dnaX*, and *atpD* housekeeping genes [32]. These set of 7 genes from: Pt679 and A4 (the latter strain was previously classified as belonging to the species *A. encheleia* based on 16S rDNA PCR-RFLP and 16S rDNA sequencing [14]), and all *Aeromonas* sp. available from NCBI RefSeq were concatenated and aligned using mafft [33] (v7.490). An unrooted maximum likelihood phylogenetic tree (Supplementary Fig. S1) was generated using IQ-TREE (2.1.4) software with bootstrap values of 1000 replicates and the '-m TEST' option to determine the best-fit substitution model.

3. Results and discussion

SDS-PAGE of lipopolysaccharides. SDS-PAGE analysis of the LPSs of *A. hydrophila* Pt679, *A. popoffii* A4 and *A. sobria* K928, which were exclusively isolated from the phenol phases from all the three strains, showed a ladder-like pattern, typical of LPS molecules of smooth bacterial cells (Fig. 1a). In the silver-stained electrophoregrams, there were both fast-migrating low-molecular-weight (LMW) R-type LPS and slow-migrating high-molecular-weight (HMW) S-type LPS species, which differed in the amount of the O-units. In addition, the analysis of very

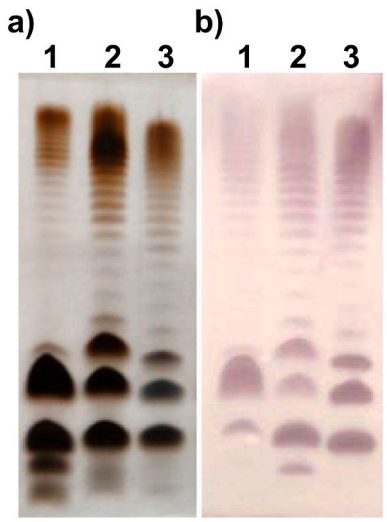

Fig. 1. Silver stained SDS-PAGE (**a**) of lipopolysaccharide samples and Western blot (**b**) with the reference PGO1 antiserum. Lanes: 1, LPS of *A. popoffii* A4; 2, LPS of *A. sobria* K928; 3, LPS of *A. hydrophila* Pt679. 3 μg were loaded per each lane.

long chain LPS fractions revealed a slightly lower degree of O-chain polymerization in the S-type LPS of *A. hydrophila* Pt679 in comparison to the corresponding fractions of *A. popoffii* A4 and *A. sobria* K928.

Serological studies of Aeromonas sp. *strains of the PGO1 serogroup.* The serotyping with agglutination tests with heat-killed bacteria and antisera of the *Aeromonas* sp. NIH scheme and additional ones for provisional serogroups revealed that *A. hydrophila* Pt679, *A. popoffii* A4, and *A. sobria* K928 strains belong to the PGO1 serogroup [2,17]. The classification to this immunotype was further confirmed in our studies by the reactivity of the PGO1 reference antiserum with LPS samples in the Western blotting and ELISA experiments.

The Western blot with the PGO1 antiserum revealed positive reactions with long-chains, semi-rough, and rough-LPS species of three *Aeromonas* strains suggesting that the cross-reactive epitope(s) are located on the entire LPS molecules (Fig. 1b), and thus confirmed the classification of the *A. hydrophila* Pt679, *A. popoffii* A4, and *A. sobria* K928 strains to the same PGO1 immunotype [17,34]. Accordingly, in the ELISA experiment (Table 1), the reference antiserum recognized LPSs of the Pt679, A4, and K928 strains. Although positive, the reactions were weaker than in the homologous system [34].

The adsorption of the PGO1 antiserum with either A4 or K928 cells sustained its reactivity only with the LPS of Pt679, however, to the lower titre after the incubation with the A4 cell biomass. Similarly, in the reverse system after adsorption of the reference antiserum with Pt679 cells, the reaction to the lower titre was sustained with A4 LPS (Table 1). These data indicated that (i) three O-antigens have common epitopes with the reference O-antigen but the similarity of Pt679 is rather higher than that of the others, (ii) the K928 and A4 O-antigens are very related to each other, and (iii) both contain a common epitope with Pt679, which is either more immunodominant in the A4 O-antigen or is not found in the K928 O-antigen.

Considering the similarities of the studied O-antigens, Western blotting and ELISA experiments with rabbit polyclonal antisera against Pt679, A4, and K928 O-serotypes in homologous and heterologous systems were performed as well. In the blots, the notable cross-reactivities of both K928 and A4 O-antisera with homologous and heterologous LPSs indicated structural similarities of these two O-antigens (Fig. 2 b,c). On the other hand, the strong positive reaction of the Pt679 O-antiserum only with the homologous S-LPS suggested higher specificity of this O-serotype (Fig. 2 a). Moreover, the reactivity within the fast-migrating R-LPS glycoforms seems to indicate similarities of the Pt679 and K928 core oligosaccharides, which was also shown by the reaction in the reverse scheme. Interestingly, the A4 antiserum recognized the R-LPS molecules of three *Aeromonas* spp. strains.

Accordingly, in the ELISA experiment (Table 1), all rabbit polyclonal antisera reacted positively with the homologous LPSs, but substantial cross-reactions were observed only for both K928 and A4 O-antisera (thus confirming the similarities of the A4 and K928 O-antigens). On the other hand, the Pt679 O-antiserum was weakly specific to the K928 and A4 LPSs; similarly, in the K928 and A4 O-antisera, there were only small fractions of antibodies that recognized structural elements within the Pt679 O-polysaccharide.

The adsorption of the K928 O-antiserum with the A4 biomass totally abolished its reactivity with all the studied LPSs, while the use of the Pt679 cells did not affect its reactivity with the homologous and A4 LPSs in the ELISA experiment (Table 1). In turn, after the adsorption of the A4 O-antiserum with the K928 biomass, the antibodies specific to the homologous A4 LPS were not completely removed, probably due to the additional structural element in the A4 LPS, which is absent in the K928 O-antigen. After the adsorption of the A4-specific serum with the Pt679 cells, its reactivity with both the homologous and K928 LPSs were

Table 1
Reactivity (reciprocal titers) of the PGO1 reference antiserum and other anti-O sera with LPSs of *Aeromonas* Pt679, A4, and K928.

Type of the antiserum	Pt679 LPS	K928 LPS	A4 LPS
anti-PGO1 [a] intact	64.000	16.000	8.000
anti-PGO1adsorbed on Pt679 cells	<1.000 [b]	4.000	2.000
anti-PGO1 adsorbed on A4 cells	8.000	<1.000	<1.000 [b]
anti-PGO1 adsorbed on K928 cells	16.000	<1.000 [b]	<1.000
anti-Pt679 intact	256.000	2.000	2.000
anti-Pt679 adsorbed on A4 cells	128.000	<1.000	<1.000 [b]
anti-Pt679 adsorbed on K928 cells	256.000	1.000 [b]	1.000
anti-A4 intact	2.000	32.000	32.000
anti-A4 adsorbed on K928 cells	<1.000	<1.000 [b]	8.000
anti-A4 adsorbed on Pt679 cells	<1.000 [b]	16.000	16.000
anti-K928 intact	4.000	256.000	128.000
anti-K928 adsorbed on A4 cells	<1.000	1.000	<1.000 [b]
anti-K928 adsorbed on Pt679 cells	<1.000 [b]	256.000	64.000

[a] the reactivity of the reference PGO1 antiserum with the cells of the reference strain was at the level of 512.000 [34].

[b] control of a proper adsorption process (efficient when the adsorbed serum did not react with the LPS of the adsorbing strain).

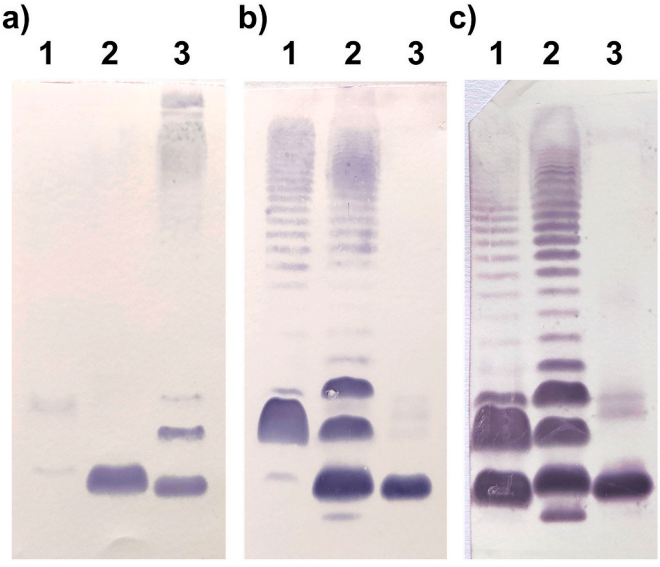

Fig. 2. Western blots of LPS samples after SDS-PAGE with polyclonal rabbit O-antisera: anti-Pt679 (**a**), anti-K928 (**b**), and anti-A4 (**c**). Lanes: 1, LPS of *A. popoffii* A4; 2, LPS of *A. sobria* K928; 3, LPS of *A. hydrophila* Pt679. 3 μg were loaded per each lane.

reduced to some extent, indicating the presence of a putative common epitope in the Pt679 and A4 O-antigens (see the next paragraph). In the reverse system, the adsorption of the Pt679 O-antiserum with either the K928 or A4 cells did not affect its reactivity with the homologous LPS, thus demonstrating that the common fragments of three O-serotypes are of little importance in the reactivity of the Pt679 O-antiserum.

Determination of the A. hydrophila Pt679 O-polysaccharide structure. The O-specific polysaccharide was obtained by mild acid hydrolysis of the LPS of *A. hydrophila* Pt679 after precipitation of lipid A and separation of the supernatant containing the carbohydrate material by GPC on a Sephadex G50 fine column. The yield of the OPS fraction was 14% of the LPS portion used for the hydrolysis. The chemical analysis of the O-polysaccharide by GLC-MS after full acid hydrolysis followed by reduction and acetylation resulted in identification of 6-deoxymannose (Rha), 2-amino-2,6-dideoxyglucose (QuiN), and 3-amino-3,6-dideoxyhexose (Fuc3N), with a peak area ratio of ~1.0 : 1.1 : 1.4. The methylation analysis of the OPS showed the presence of 2,3-di-*O*-methyl-6-deoxyhexitol-1-*d* (derived from 4-substituted Rha), 2,4-di-*O*-methyl-6-deoxyhexitol-1-*d* (derived from 3-substituted Rha), 4-*O*-methyl-6-deoxyhexitol-1-*d* (derived from 2,3-disubstituted Rha), 2,6-dideoxy-4-*O*-methyl-2-(*N*-methyl)acetamidohexitol-1-*d* (derived from 3-substituted QuiN), and 3,6-dideoxy-2,4-di-*O*-methyl-3-(*N*-methyl) acetamidohexitol-1-*d* (derived from terminal Fuc3N), with a peak area ratio of ~1.2 : 1.0 : 1.3 : 3.0 : 2.4, identified by GLC-MS.

The determination of the absolute configuration of the monosaccharides by GLC of the acetylated (*S*)-(+)-2-octyl glycosides and comparison with authentic standards [24] showed the L configuration of Rha and the D configuration of QuiN. The D configuration of Fuc3N was determined by the analysis of the ^{13}C glycosylation effects in the OPS.

The ^{1}H NMR spectrum of the O-polysaccharide (Fig. 3) showed five major signals for anomeric protons at δ 5.10, 4.95, 4.92, 4.85, and 4.77, with an integral intensity ratio of 1.0 : 1.0 : 1.2 : 1.1 : 1.2, five C*H*$_3$–CH groups of 6-deoxyhexoses in the range of δ 1.25–1.37, two signals for *N*-acetyl groups at δ 2.08, and ring proton signals in the range of δ 3.26–4.54; some of the signals overlapped.

Homo- and heteronuclear 2D NMR experiments (^{1}H,^{1}H DQF-COSY, TOCSY, NOESY, ^{1}H,^{13}C HSQC, and ^{1}H,^{13}C HMBC) were performed to assign all the spin systems and to establish the sugar sequence in the O-antigen repeating unit. Both the absence of signals in the region of δ 84.0–88.0 characteristics of C-4 furanoses and the anomeric carbon resonances, which should have higher chemical shift values due to the less shielded nuclei than in their configurationally related counterparts, demonstrated that all the sugars were pyranoses [35]. In the ^{1}H,^{13}C HSQC spectrum (Fig. 4), two correlation signals at δ 4.18/52.0 and 3.85/56.9 of the protons at the nitrogen-bearing carbons to the corresponding carbons and five H-6/C-6 signals in the range of δ 1.25–1.37/16.4–18.0 were found, which showed that two of the five monosaccharides building the OPS of Pt679 were *N*-acetamido sugars. The ^{1}H and ^{13}C NMR chemical shifts are collected in Table 2.

The anomeric configuration of each monosaccharide was assigned on the basis of $^{3}J_{H1,H2}$ and $^{1}J_{C1,H1}$ coupling constants, whereas the values of the vicinal $^{3}J_{H,H}$ sugar ring coupling constants allowed identification of the configuration of each sugar residue.

In the ^{1}H, ^{1}H TOCSY spectrum, the correlations of the ring protons with H-6 methyl protons were observed for the **A**, **D,** and **E** spin systems, which were recognized as *manno*pyranoses on the basis of the vicinal $^{3}J_{H,H}$ coupling constant values: $^{3}J_{1,2}$ (~2 Hz), $^{3}J_{2,3}$ (3 Hz), $^{3}J_{3,4}$ (8.5 Hz), $^{3}J_{4,5}$ (~9 Hz), and $^{3}J_{5,6}$ (6 Hz) [36]. However, some proton signals overlapped, i.e. H-2 and H-3 of residue **D** and H-4 and H-5 of residue **E**. The long range correlations observed for the H-1 and H-6 protons in the HMBC spectrum were useful to completely assign the Rha*p* carbon atoms, and then some coinciding proton signals were distinguished after the analysis of the ^{1}H,^{13}C HSQC spectrum (Fig. 4). The data of the methylation analysis and the effect of glycosylation on chemical shifts of the carbon atoms were also taken into account.

The α-configuration of residues **A** and **D** and the β-configuration of residue **E** were assigned by the $^{1}J_{C1,H1}$ values of 176, 173, and 163 Hz, respectively. Furthermore, the chemical shifts of C-5 for the **A** and **D** sugars at δ 70.7 and 68.6, respectively, demonstrated that they were α-Rha*p*, whereas residue **E** was β-Rha*p* (δ 73.2), in comparison with the chemical shifts of δ 70.0 and 73.0 for C-5 in α-Rha*p* and β-Rha*p*, respectively [14,37,38].

In the ^{1}H,^{1}H TOCSY spectrum, correlations of the H-1 signal with H-2, H-3, and H-4 were found and indicated that spin system **B** was a sugar residue with the *galacto* configuration. The H-5 and H-6 proton signals were assigned from the H-3/H-5, H-4/H-5, and H-4/H-6 correlations observed in the ^{1}H,^{1}H NOESY spectrum. In the ^{1}H,^{13}C HSQC spectrum (Fig. 4), the correlation signal at δ 4.18/52.0 (H-3/C-3) of the proton at the nitrogen-bearing carbon to the corresponding carbon and the H-6/C-6 signal at δ 1.25/16.4 were assigned to spin system **B**. The presence of the *N*-acetylated group was confirmed by the long range correlations in the HMBC spectrum of H-3 **B** with the carbonyl carbon of the acetyl group at δ 4.18/175.5 and of the latter with the methyl group at δ 2.08. The α-anomeric configuration of the residue was inferred from the $^{3}J_{H1,H2}$ and $^{1}J_{C1,H1}$ coupling constant values of 3 Hz and 173 Hz, respectively. These data allowed identification of spin system **B** as α-Fuc3N.

All the ^{1}H resonances of spin system **C** were assigned from the ^{1}H,^{1}H COSY and confirmed by the correlations from the ^{1}H,^{1}H TOCSY

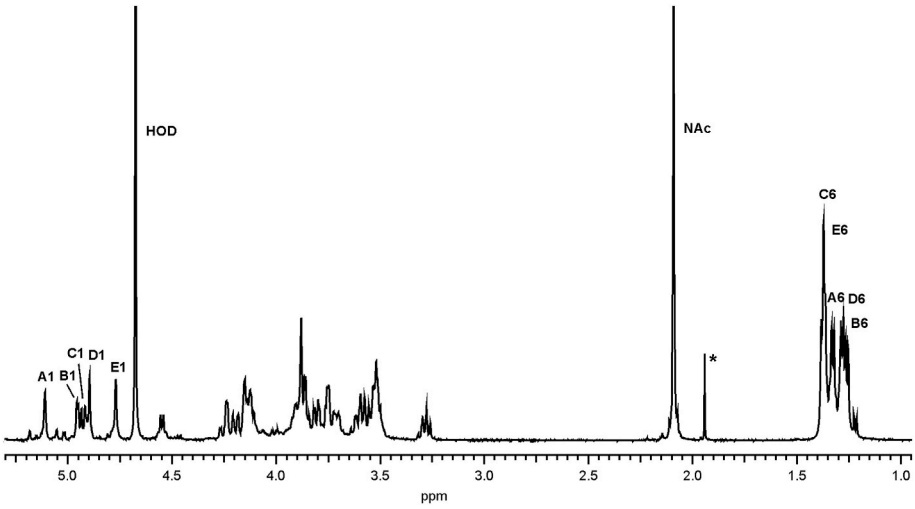

Fig. 3. ^{1}H NMR spectrum of the OPS of *A. hydrophila* strain Pt679. The spectrum was recorded at 32 °C in D_2O at 500 MHz. The capital letters and Arabic numerals refer to atoms in the sugar residues denoted as shown in Table 2. NAc - N-acetyl group, asterisk - free acetic acid.

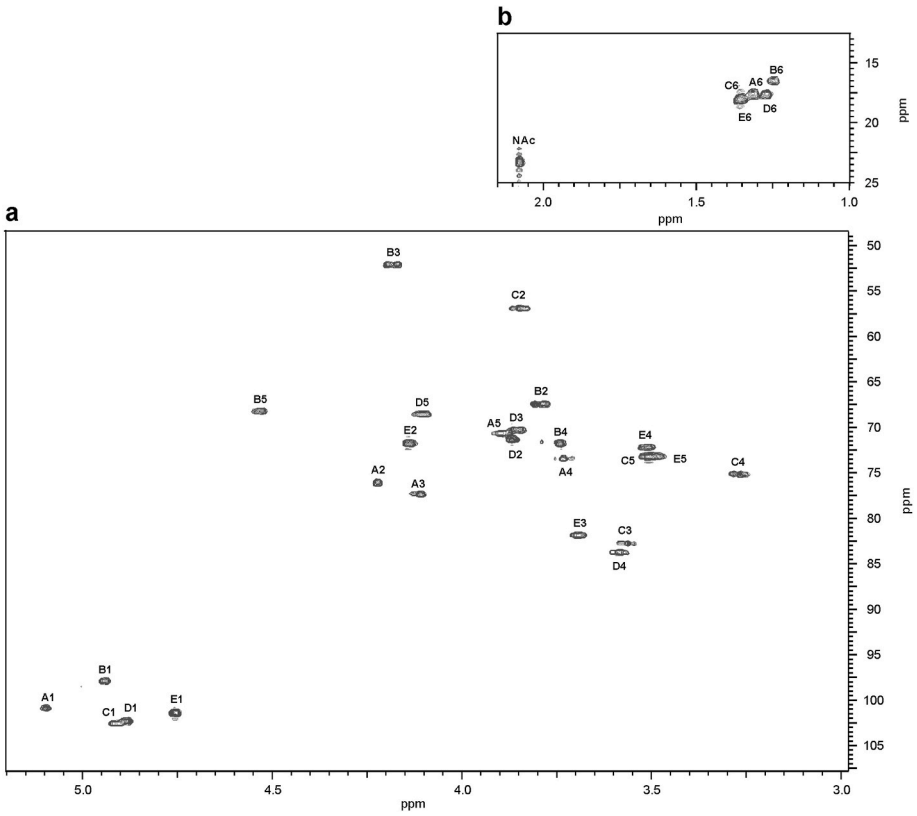

Fig. 4. $^{1}H,^{13}C$ HSQC (500 × 125 MHz) spectrum of the OPS of *A. hydrophila* strain Pt679.
The parts represent: (**a**) the anomeric region and the region for the ring atoms; (**b**) the region for the methyl groups of 6-deoxy sugars and an N-acetyl group. The spectrum was recorded at 32 °C in D_2O as a solvent. The capital letters and Arabic numerals refer to proton/carbon pairs in the respective sugar residues denoted as shown in Table 2.

Table 2
^{1}H (500.4 MHz) and ^{13}C NMR (125 MHz) data (δ, ppm) for the OPS of *A. hydrophila* strain Pt679.

Sugar residue		H-1 C-1	H-2 C-2	H-3 C-3	H-4 C-4	H-5 C-5	H-6 C-6	NAc
→2,3)-α-L-Rha*p*-(1→ $^{1}J_{C,H}$ = 176 Hz	**A**	5.10,100.8	4.22 76.2	4.12 77.4	3.73 73.4	3.90 70.7	1.32 17.6	
α-D-Fuc*p*3NAc-(1→ $^{1}J_{C,H}$ = 173 Hz	**B**	4.95 97.8	3.79 67.4	4.18 52.0	3.74 71.8	4.54 68.3	1.25 16.4	2.08 23.3; 175.5
→3)-β-D-Qui*p*NAc-(1→ $^{1}J_{C,H=}$164 Hz	**C**	4.92,102.6	3.85 56.9	3.56 82.8	3.26 75.2	3.51 73.2	1.37 18.0	2.08 23.3; 175.2
→4)-α-L-Rha*p*-(1→ $^{1}J_{C,H}$ = 173 Hz	**D**	4.89,102.3	3.86 71.4	3.87 70.4	3.58 83.8	4.11 68.6	1.27 17.6	
→3)-β-L-Rha*p*-(1→ $^{1}J_{C,H}$ = 163 Hz	**E**	4.77,101.4	4.14 71.8	3.69 81.9	3.52 72.4	3.51 73.2	1.36 18.0	

spectrum. Based on the high value of the ring proton coupling constants (~10 Hz), as expected for the *gluco* configuration combined with the H-2/C-2 and H-6/C-6 correlations at δ 3.85/56.9 and 1.37/18.0, respectively, observed in the $^{1}H,^{13}C$ HSQC spectrum (Fig. 4), spin system **C** was assigned to Qui*p*N. The $^{1}J_{C1,H1}$ and $^{3}J_{H1,H2}$ values of 164 and 8.5 Hz, respectively, showed the β-anomeric configuration of this residue.

The displacement of carbon atom signals C-2 (δ 76.2) and C-3 (δ 77.4) of spin system **A**, C-3 of the **C** (δ 82.8) and **E** (δ 81.9) spin systems, and C-4 (δ 83.8) of spin system **D**, compared with their positions in the corresponding non-substituted monosaccharides [39], confirmed the glycosylation pattern of the monosaccharides in the OPS repeating unit. In turn, the insignificant downfield shift of the signals for carbons C-2,3, 4,6 of spin system **B** [38,40,41] indicated a terminal position of this sugar in the OPS.

In the $^{1}H,^{13}C$ HMBC spectrum (Fig. 5), there were correlations between anomeric protons and transglycosidic carbons: Rha*p* **A** H-1/Rha*p* **E** C-3 at δ 5.10/81.9, Rha*p* **E** H-1/Rha*p* **D** C-4 at δ 4.77/83.8, Rha*p* **D** H-1/Qui*p*NAc **C** C-3 at δ 4.89/82.8, Qui*p*NAc **C** H-1/Rha*p* **A** C-3 at δ 4.92/77.4, and Fuc*p*3NAc **B** H-1/Rha*p* **A** C-2 at δ 4.95/76.2. Furthermore, the following correlations between anomeric carbons and transglycosidic protons were also visible in the spectrum: Rha*p* **A** C-1/Rha*p* **E** H-3 at δ 100.8/3.69, Rha*p* **E** C-1/Rha*p* **D** H-4 at δ 101.4/3.58, Rha*p* **D** C-1/Qui*p*NAc **C** H-3 at δ 102.3/3.56, Qui*p*NAc **C** C-1/Rha*p* **A** H-3 at δ 102.6/4.12, and Fuc*p*3NAc **B** C-1/Rha*p* **A** H-2 at δ 97.8/4.22.

The $^{1}H,^{1}H$ NOESY spectrum (Fig. 6) showed correlations for pairs of transglycosidic protons, i.e. **A** H-1,**E** H-3; **E** H-1,**D** H-4; **D** H-1,**C** H-3; **C** H-1,**A** H-3; **B** H-1,**A** H-2 at δ 5.10/3.69; 4.77/3.58; 4.89/3.56; 4.92/4.12, and 4.95/4.22, respectively. These data confirmed the monosaccharide sequence in the OPS defined by the heteronuclear $^{1}H,^{13}C$ HMBC experiment. Additionally, the NOESY spectrum (Fig. 6) showed intra-residue cross-peaks, which confirmed the anomeric configuration of the sugar residues. There were correlations between H-1/H-2 for α-Rha*p* (**A** and **D**); H-1/H-2, H-1/H-3, and H-1/H-5 for β-Rha*p* (**E**); H-1/H-2 for α-Fuc*p*3N (**B**), and H-1/H-3 and H-1/H-5 for β-Qui*p*N (**C**).

The analysis of the glycosylation effects on the ^{13}C NMR chemical shifts allowed establishing the absolute configuration of Fuc*p*3N (**B**). In the disaccharide fragment **B**-(1 → 2)-**A**, α-Fuc*p*3N-(1 → 2)-α-L-Rha*p*, the small positive α-effect on C-1 of residue **B** (+5.7 ppm) and C-2 of residue **A** (+4.1 ppm) indicated different D-L absolute configurations of the linked monosaccharides. In the case of the same L-L absolute configurations, the positive α-effect on C-1 of residue **B** and C-2 of residue **A** would have been much higher: >8.1 ppm and >8.2 ppm, respectively [40,42]. These data confirmed the D absolute configuration of α-Fuc*p*3N.

Based on the results obtained, it was concluded that the OPS of *A. hydrophila* Pt679 is composed of a branched pentasaccharide repeating unit and contains three Rha*p* (**A**, **D**, **E**) and one Qui*p*NAc (**C**) in

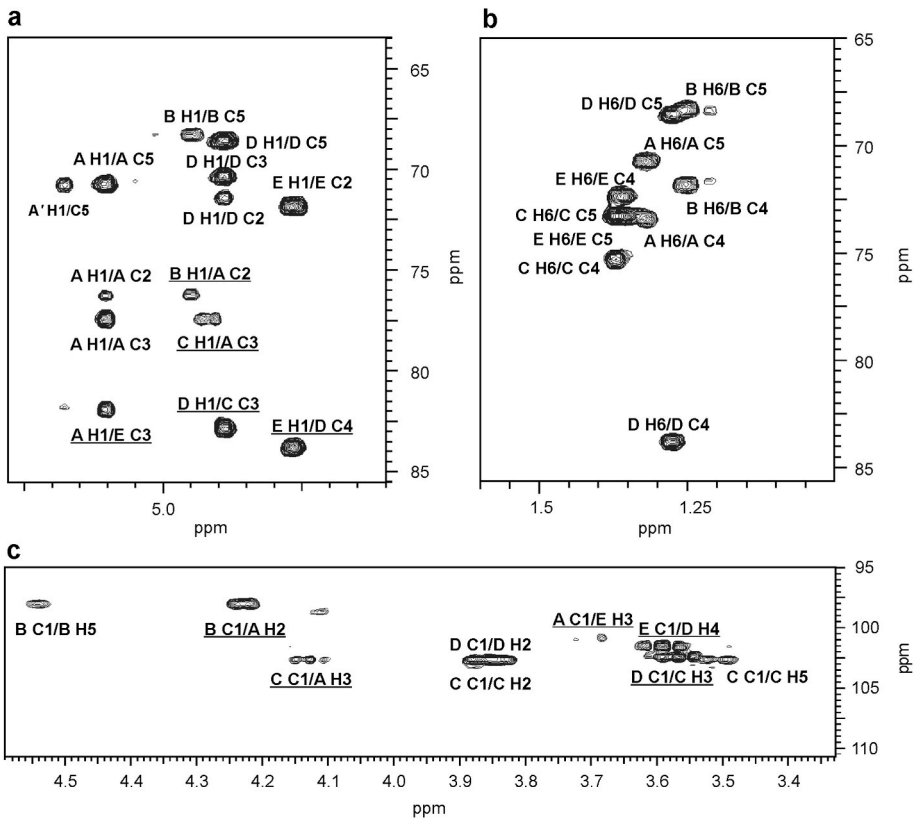

Fig. 5. Regions of the $^{1}H,^{13}C$ HMBC spectrum of the OPS of *A. hydrophila* strain Pt679. The long-range heteronuclear correlations for (**a**) anomeric protons, (**b**) H-6 protons, and (**c**) anomeric carbons are marked. Inter-residue correlations important for establishing the sugar sequence in the O-antigen repeating unit are underlined. The capital letters and Arabic numerals refer to atoms in the sugar residues denoted as shown in Table 2. A′H1/C5 at δ 5.17/70.7 represents the α-L-Rha*p* correlation signal of the shorter-chain fraction of the OPS or the fraction without substitution with a terminal Fuc3N residue; however, only few ^{1}H and ^{13}C resonances have been found.

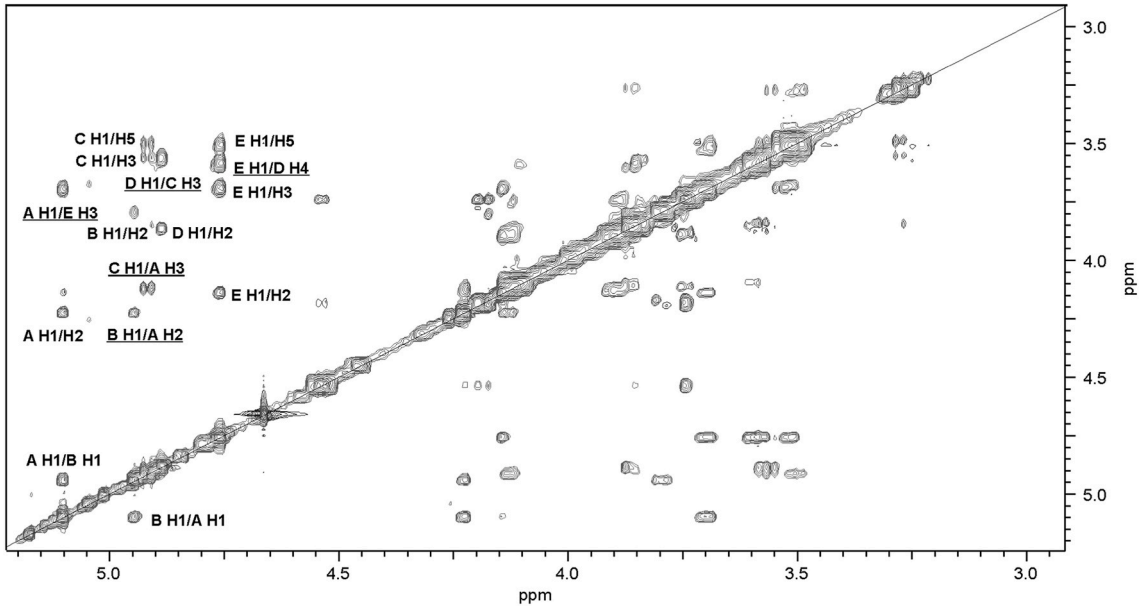

Fig. 6. Part of $^{1}H,^{1}H$ NOESY spectrum of the OPS from *A. hydrophila* strain Pt679. The NOE correlations between anomeric protons and protons at the glycosidic linkages are underlined. Some other important H/H correlations are depicted as well. The capital letters and Arabic numerals refer to protons in the sugar residues denoted as shown in Table 2.

the linear part and Fuc3NAc (**B**) located at the terminal position and glycosylating the α-Rha*p* residue (**A**) at carbon C-2.

The structure of the O-antigen of *A. hydrophila* strain Pt679 is unique among known bacterial O-polysaccharides; however, there are some common elements in the composition with the recently published O-polysaccharides of *A. popoffii* A4 and *A. sobria* K982 [14,15] classified to the same provisional serogroup PGO1. The similarities concern the general structure of the repeating unit, which is a branched pentasaccharide (Fig. 7). The difference between the O-polysaccharides lies in one sugar, i.e. β-D-Qui*p*NAc, which is replaced by β-D-Fuc*p*NAc in the O-polysaccharide of *A. sobria* K928 [15]. Moreover, three O-antigens contain α-D-Fuc3N located in the side chain; however, in both A4 and K928 OPS, this residue contains an N-linked (*R*)-3-hydroxybutanoyl (Fuc3N*R*Hb) group, whereas in the OPS studied here the sugar is

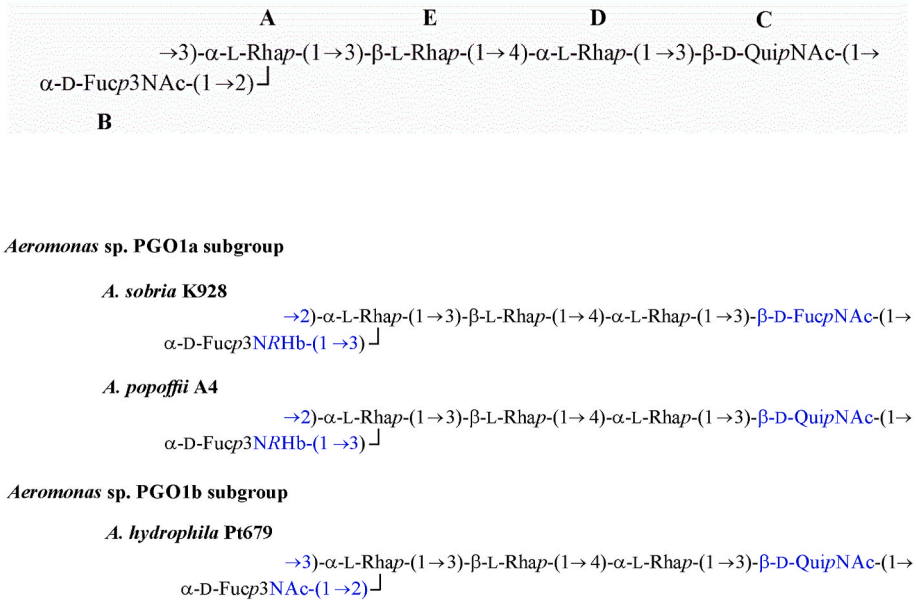

Fig. 7. Scheme of the O-antigen repeating units of *A. hydrophila* Pt679, *A. popoffii* A4 [14], and *A. sobria* K928 [15] strains classified to the PGO1 serogroup. Structural elements and linkages that differentiate the O-units are marked in blue. Representatives of the *Aeromonas* sp. PGO1a and PGO1b subgroups are indicated.

N-acetylated. Additionally, the difference concerns the position of glycosylation of disubstituted α-Rha*p* by α-D-Fuc3N at C-3 or C-2 in the OPS of *A. popoffii* A4 and *A. sobria* K928 and *A. hydrophila* Pt679, respectively (Fig. 7). It can be assumed that the terminal position of α-D-Fuc3N and its non-carbohydrate substituent is essential for the immunospecificity of *Aeromonas* spp. strains classified into the PGO1 serogroup.

Characterization of the A. hydrophila Pt679 O-antigen gene cluster. The draft genome sequence of *A. hydrophila* Pt679 contains 105 contigs with the mean coverage of ~96x, a genome size of 4,696,737 bp, and GC content of 61.63%. The O-antigen gene cluster of 23,869 bp contains 20 open reading frames *orf* (designated as *orf1* – *orf20*) with tentatively assigned function, including housekeeping genes, nucleotide sugar synthesis genes, glycosyltransferase genes, and O-antigen processing genes, whose functions have been assigned based on their similarity to genes from the databases (NCBI nr/nt, InterPro-related databases, KEGG) (Table 3).

The *orf1* and *orf2* share 100% identity with *acrB* and *oprM* housekeeping genes encoding the multidrug pump subunit and the outer membrane protein, respectively. Similar location at the 3'-end was also found in *A. hydrophila* O13 and O33 O-antigen gene clusters [30]. In Pt679 OGC, there are four *rml* genes (*orf3-6*) in the order *rmlBDAC* located downstream of both housekeeping genes, which based on the high identity of 81–95% to *E. coli rml* genes were proposed to catalyse the synthesis of dTDP-L-rhamnose ([cited 2023 May 20]. Available from: https://www.ncbi.nlm.nih.gov/).

Orf7,8 and *9* share 100% identity with *fdtA*, *fdtC*, and *fdtB* of *A. hydrophila*, whose products are known to be engaged in the dTDP-D-Fuc3N synthesis pathway. However, the first two steps of the process require RmlA and RmlB activities, followed by isomerase FdtA and transaminase FdtB catalyzing the synthesis of dTDP-D-Fuc3N. Finally, N-acetyltransferase FdtC is responsible for the transfer of an acetyl group to dTDP-D-Fuc3N to form dTDP-D-Fuc3NAc [43–45]. Two genes: *orf16* and *orf18* encode putative homologs of NAD-dependent epimerase/dehydratase and are involved in the biosynthesis of D-QuiNAc. They share 49% (*orf18*) and 39% (*orf16*) identity with WbpM and WbpV/WbpK of *Pseudomonas aeruginosa* PAO1 [46,47]. WbpM is a UDP-D-GlcNAc 4,6-dehydratase converting UDP-D-GlcNAc into UDP-4-keto-D-QuiNAc, whose intermediate is then processed by WbpV to form UDP-D-QuiNAc or by WbpK to form UDP-D-FucNAc [47].

There are four putative glycosyltransferase genes (*orf11,13,14,15*) for the Pt679 O-unit assembly, as was predicted by the high identity level to glycosyltransferases class 2 of *Vibrio* spp., *Shigella* spp., and *Aeromonas* spp. The o*rf13*-encoded protein shares 37% identity with WbsW of *Vibrio parahaemolyticus*, whereas *orf14* and *orf15*-encoded proteins exhibit 58% and 48% identity with WbsX and WbsY glycosyltransferases of *S. boydii* O11, respectively. These three *orfs* can be proposed to encode putative rhamnosyltransferases.

The *orf11* gene was identified as encoding the glycosyltransferase 4 family protein with 43% identity and 64% similarity to *wekP* (a *wegP* synonym) glycosyltransferase. Given the localization of the gene between *wzx* and *wzy* in the studied OGC, similarly to the position of *wekP* of *E. coli* O2, and taking into account that the enterobacterial O-antigen also contains terminal D-Fuc3NAc, it seems that the *orf11* gene encodes putative D-Fuc3NAc transferase [37,48].

The *orf17* gene shares 90% identity with an undecaprenyl-phosphate beta-N-acetyl-D-fucosamine-phosphotransferase (*GT1*) and is located upstream of *wzz*, similarly as in the *A. sobria* K928 OGC [15]. The *GT1* may be thus responsible for initializing the sequential O-unit synthesis by transfer of the sugar from a corresponding nucleotide precursor to a membrane-linked undecaprenyl phosphate carrier [49]. However, unlike in the K928 OGC, in the region studied here, *GT1* results in the formation of Und-PP-D-QuiNAc instead of Und-PP-D-FucNAc, which is almost certainly the initial sugar for the Pt679 O-unit assembly.

Besides the *orf15*-encoded rhamnosyltransferase responsible for the formation of the L-Rha-α-(1 → 3)-L-Rha disaccharide structural element, analogously to the function of WbsY of *S. boydii* O11, with whom it shows 48% identity, the other glycosyltransferases were not assigned to the linkages, but their total number in the Pt679 OGC is in full agreement with expected for the pentasaccharide O-unit.

Orf10, 12, 19, and *20* are proposed to be genes facilitating the Wzx/Wzy biosynthesis pathway [50]. The *orf10* gene has 100% identity to the O-antigen translocase (Wzx) of *A. hydrophila*. The *orf12* gene shares 100% identity to the *A. hydrophila* EpsG family protein, which includes the O-antigen polymerase, and 37% identity to Wzy of *Shigella boydii.* Additionally, the *orf10* and *orf12*-encoded proteins contain 12 and 11 predicted transmembrane segments (TMS), which are typical numbers for flippase (Wzx) and polymerase (Wzy), respectively. *Orf19* and *orf20* share high identity (98–100%) to the Wzz/FepE/Etk N-terminal domain-containing protein of *A. hydrophila* and the O-antigen ligase

Table 3
Characteristics of the *orfs* in the *A. hydrophila* strain Pt679, serogroup PGO1 O-antigen gene cluster.

orf no.	Gene	Gene position in OGC sequence	No of aa	G + C content [%]	Similar protein(s) (strain, GenBank Accession No.)	% Identical/% similar (no. of aa overlap)	Putative function of protein
1	*acrB*	0–3150	1049	63.3	efflux RND transporter permease subunit, *Aeromonas* (WP_029299709.1)	100/100 (1049)	Multidrug efflux pump subunit AcrB
					efflux RND transporter permease AcrB, Enterobacteriaceae (WP_001132469.1)	69/83 (1007)	
2	*oprM*	3142–4552	469	25.2	efflux transporter outer membrane subunit, *Aeromonas hydrophila* (WP_252450504.1)	100/100 (465)	Outer membrane protein OprM
					outer membrane protein OprM, *Aeromonas hydrophila* (AID71060.1)	98/98 (465)	
3	*rmlB*	5254–6340	361	32.9	dTDP-glucose 4,6-dehydratase, *Aeromonas hydrophila* (WP_242798213.1)	99/99 (358)	dTDP-d-glucose-4,6-dehydratase
4	*rmlD*	6339–7227	295	28.6	dTDP-4-dehydrorhamnose reductase, *Aeromonas hydrophila* (WP_252453897.1)	100/100 (293)	dTDP-4-dehydrorhamnose reductase
5	*rmlA*	7339–8218	292	38.8	glucose-1-phosphate thymidylyltransferase RfbA, *Aeromonas hydrophila* (WP_252453895.1)	100/100 (290)	Glucose-1-phosphate thymidylyltransferase
6	*rmlC*	8277–8820	180	51.6	dTDP-4-dehydrorhamnose 3,5-epimerase, *Aeromonas caviae* (WP_214003767.1)	96/97 (179)	dTDP-4-dehydrorhamnose 3,5-epimerase
7	*fdtA*	8823–9240	139	37.2	FdtA/QdtA family cupin domain-containing protein, *Aeromonas hydrophila* (WP_252452602.1)	100/100 (139)	dTDP-6-deoxy-3,4-keto-hexulose isomerase
8	*fdtC*	9220–9679	153	39.9	N-acetyltransferase, *Aeromonas hydrophila* (MBX9564203.1)	100/100 (153)	N-acetyltransferase
9	*fdtB*	9683–10787	367	31	DegT/DnrJ/EryC1/StrS family aminotransferase, *Aeromonas hydrophila* (WP_252452605.1)	100/100 (364)	Aminotransferase (dTDP-3-amino-3,6-dideoxy-alpha-d-galactopyranose transaminase)
10	*wzx*	10783–12034	416	37.8	O-antigen translocase, *Aeromonas hydrophila* (WP_252452608.1)	100/100 (412)	Flippase
11	*wegP/ wekP*	12062–13103	346	41.5	glycosyltransferase family 4 protein, *Escherichia coli* O2 (AQU71802.1)	43/64 (336)	Glycosyltransferase class 4
12	*wzy*	13119–14169	349	41.7	Wzy, *Shigella boydii* (AAS98031.1)	37/53 (343)	Polymerase
					EpsG family protein, *Aeromonas hydrophila* (WP_252452614.1)	100/100 (346)	
13	*wbsW*	14202–15018	271	42.3	WbsW, *Vibrio parahaemolyticus* (QFF90337.1)	37/57 (263)	Glycosyltransferase class 2
					WbsW, *Shigella boydii* (AAS98032.1)	31/55 (220)	
					Glycosyltransferase, *Aeromonas* sp. MR16 (WP_241343263.1)	45/64 (267)	
14	*wbsX*	15035–16163	375	26.4	WbsX, *Shigella boydii* O11 (AAS98033.1)	58/73 (368)	Glycosyltransferase
15	*wbsY*	16168–17068	299	44.7	WbsY, *Shigella boydii* O11 (AAS98034.1)	48/67 (293)	Glycosyltransferase class 2
					Glycosyltransferase, *Aeromonas caviae* (WP_010675326.1)	97/97 (297)	
16	*wbpV*	17083–18046	320	39.5	WbpK, *Pseudomonas aeruginosa* PAO1 (AAC45865.1)	39/55 (307)	NAD-dependent epimerase/dehydratase /UDP-galactose-4-epimerase
					NAD-dependent epimerase/dehydratase family protein, *Aeromonas caviae* (WP_236752775.1)	100/100 (317)	
17	*GT1*	18039–18597	185	34.9	Undecaprenyl-phosphate beta-N-acetyl-d-fucosamine-phosphotransferase, *Aeromonas hydrophila* (BDC81682.1)	90/94 (185)	Undecaprenyl-phosphate beta-N-acetyl-d-quinovosamine-phosphotransferase
					Lipid carrier-UDP-N-acetyl-galactosaminyltransferase, *Aeromonas caviae* (OCW45364.1)	94/96 (182)	
18	*wbpM*	18656–20618	653	42.2	WbpM, *Pseudomonas aeruginosa* (AAF23989.1)	49/66 (621)	Nucleotide sugar epimerase/dehydratase
					nucleoside-diphosphate sugar epimerase/ dehydratase, *Aeromonas hydrophila* (WP_252452629.1)	100/100 (647)	
19	*wzz*	20971–22042	356	22.1	Wzz/FepE/Etk N-terminal domain-containing protein, *Aeromonas hydrophila* (WP_252452631.1)	100/100 (353)	O-antigen chain length determinant protein
20	*waaL*	22153–23869	571	40.4	O-antigen ligase C-terminal domain-containing protein, *Aeromonas hydrophila* (EIS3737982.1)	98/98 (554)	Ligase

C-terminal domain-containing protein of *A. hydrophila*; thus, they have been identified as Wzz (O-antigen length determinator) and WaaL, respectively. Putative WaaL contains twelve TMS and is involved in ligation of the O-antigen to the lipid A/core.

Characterization of the A. popoffii A4 O-antigen gene cluster. The OGC of *A. popoffii* A4 with the genome size of 4,527,665 bp, and GC content of 58.74%, is 20,025 bp long and contains 19 annotated open reading frames (*orfs*) (Supplementary Table S1). Unlike the Pt679 and K928 O-antigen gene clusters [15], which are mapped downstream of both *oprM* and *acrB* housekeeping genes or between them, respectively, the OGC of *A. enecheleia* A4 seems not to be flanked or preceded by any conserved genes. Instead, at the 5′- and 3′-end of the sequence, homologs of *rmlB* and *waal* have been found, respectively. While WaaL-encoding *orf* has been found to occur at the 3′-end of some *A. hydrophila* OGC studied so far [30], the position of *rmlB* in *Aeromonas* OGC is shown for the first time; however, a similar deficiency of housekeeping genes has been identified in e.g., *Salmonella* O11, O42, and O59 O-antigen gene clusters [51]. In the OGC of A4, there are four (*orf 1–4*) homologs of *rmlBDAC* genes involved in dTDP-L-Rha synthesis. They share identity in the range of 83–97% with the enterobacterial *rml* gene set. *Orf5, 6,* and *8*, which showed 95–97% identity with the *fdtA*, *fdhC*, and *fdtB* genes of *A. veronii* and *A. hydrophila* were assigned as the genetic determinants of enzymes putatively involved in Fuc3NR3Hb synthesis. The OGC of *A. enecheleia* A4 includes five putative glycosyltransferase genes assigned based on the high identity level with the GTs of *S. boydii* and *V. parahaemolyticus*. *Orf10* and *orf13* encode GT2 and WbsX, respectively, and *orf12* and *orf14* encode glycosyltransferases class 2: WbsW and WbsY, respectively. *Orf16* share 94% identity to GT1 of K928 and can be tentatively assigned to the initial transferase. The *orf9*, *orf11*, *orf18*, and *orf19* genes are assigned to Wzx/Wzy-pathway genes and identified as Wzx, Wzy, Wzz, and WaaL, respectively, based on amino acid similarities in the range of 90–98% and 35% (Wzy).

Comparison of the Aeromonas PGO1 serogroup OGCs. To elucidate the genetic basis of the O-antigen structural similarities in the three *Aeromonas* strains, the OGC sequences of Pt679 and A4 (Supplementary Table S2, Fig. 8) were compared with the recently annotated region of *A. sobria* K928 [15]. The A4 and Pt679 OGCs were found to share identity for the corresponding proteins in the range of 67–98% and 64–98%, respectively. Lower homology of 44% and 38% was found for Wzz of both A4 and Pt679 and WbsW of Pt679, respectively. The unique protein sequence was represented by Wzy of Pt679, whereas the O-antigen polymerases of A4 and K928 showed a high identity level of 84%. Although these three strains were classified to the same serogroup PGO1, which seems to be related to the high structural similarity of their O-antigens, differences were found between them. The chemical studies have shown that the common structural elements are accompanied by specific ones whose phenotypic representation requires genes for their synthesis. Since all the three strains contain branched pentasaccharide O-repeating units, where the D-Fuc3N residue has the terminal position, the homologs of *fdtA*, *fdtB*, and *fdtC* genes determining the synthesis of dTDP-D-Fuc3N are found in their OGCs. There are two different derivatives of the 3-amino-3,6-dideoxygalactose, i.e. N-acetylated D-Fuc3N in the O-antigen of Pt679 and decorated with the amido-linked 3-hydroxybutanoyl group, in both A4 and K928 O-polysaccharides; therefore, there should also be differences at the genetic level. The DNA sequences of *fdtC* (*orf8*) of Pt679 and *fdtC* (*orf7*) of K928 do not share high identity and similarity levels and thus possibly participate in the synthesis of two different sugars: dTDP-D-Fuc3NAc and dTDP-D-Fuc3NRHb, respectively. Therefore, we proposed to assign the *orf8* of Pt679 OGC to *fdtC* encoding dTDP-D-Fuc3N acetyltransferase (FdtC), due to the similarity of this gene to *Salmonella* O55 *fdtC* [51,52]. On the other hand, considering its function as putative butyryltransferase, the *orf7* of K928 OGC should be annotated with *fdhC*. In the literature, the abbreviation *fdhC* is adopted rather for a gene that encodes 3-hydroxybutanoyl transferase, responsible for the formation of dTDP-D-Fuc3NRHb. The *fdhC*-encoded transferase of *E. coli* O103:H2 carries out an analogous reaction (FdhC/WbtB [53]) and is known as a homolog of this gene (*E. coli* O103 [45,51]). Moreover, the *fdtC*

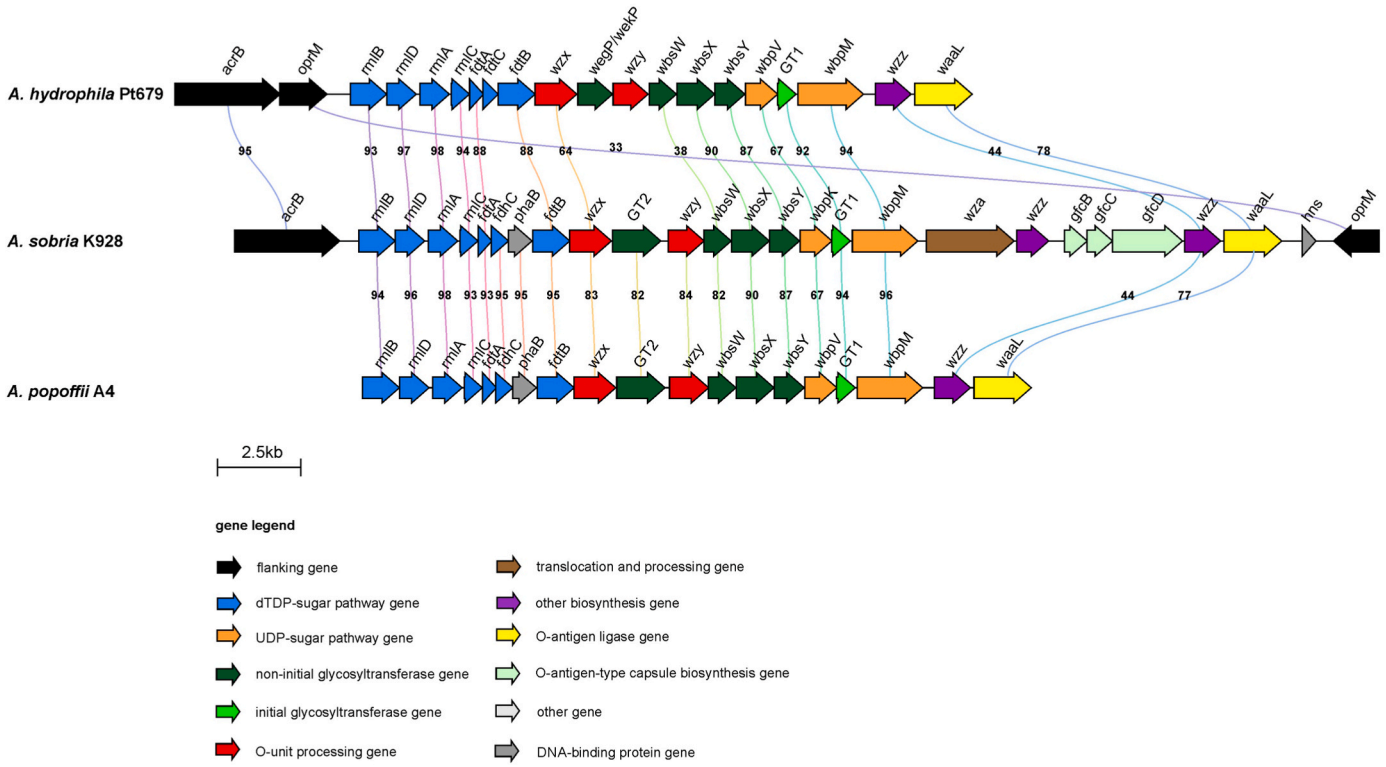

Fig. 8. Comparison of the O-antigen gene clusters of *A. hydrophila* Pt679, *A. popoffii* A4, and *A. sobria* K928 [15] classified to the same PGO1 serogroup. Amino acid identities (%) are shown on the line connecting the corresponding genes. The visualization of the OGC regions was generated by Clinker [31].

designation is rather reserved for the *orf*-encoded N-acetyltransferase, which catalyses the transfer of an acetyl group to D-Fuc3N to form dTDP-D-Fuc3NAc as the final product [44]. In the graphical representation of the OGC regions, such designations were applied for the genes (Fig. 8). Although D-QuiNAc and D-FucNAc are synthesised as UDP-sugars from UDP-GlcNAc in a combined pathway, in both cases WbpM initiates the process and then the synthesis diverges, and either WbpV or its homolog WbpK is involved, leading to formulation of UDP-D-QuiNAc and UDP-D-FucNAc, respectively. The former situation is found in Pt679 and A4, and the latter in K928, and both phenotypes have been confirmed by the content of the corresponding OGCs.

The length of the OGC regions in the genomes of the *Aeromonas* PGO1 serogroup correlates with the gene cluster loading. This observation is supported by the fact that no homologs of several genes, i.e. *wza*, *gfcB*, *gfcC, gfcD*, *hns*, and *oprM*, were found in the Pt679 and A4 OGCs, and thus these clusters are shorter than that in the K928 OGC. The deficiency concerns genes encoding proteins for the O-antigen–type capsule assembly (*gfcB*, *gfcC*, *gfcD*), histone-like nucleoid structuring protein (*hns*), and outer membrane protein *oprM* (in *A. popoffii* A4 OGC). Since not all *A. hydrophila* OGCs include these genes, it seems that they are not key genes for the O-antigen formation [30]. However, the *gfcBCD* operon preceded by the *wza* and *wzz*, with the latter gene representing the second functional copy encoding the O-antigen chain length determinator (Fig. 8), may contribute to the higher virulence of *A. sobria* K928 [15]. The pathogenic potential of the bacterial strain that correlated with the expression of the O-antigen–type capsule was characteristic of *A. hydrophila* ML09-119, responsible for epidemic MAS outbreaks in catfish [54].

4. Conclusion

The serological experiments (Western blotting and ELISA) with the PGO1 antiserum indicated that the three studied O-antigens share structural elements with the reference O-antigen, whose structure however remains unknown, but the similarity of Pt679 is rather higher than the others. In turn, the K928 and A4 O-antigens are strongly related to each other, and the latter one contains a common epitope, i.e. 3-substituted β-D-QuiNAc with Pt679.

The studies with polyclonal antisera (anti-Pt679, A4, and K928) revealed that the occurrence of the common linear L-Rha*p* trisacchride within branched pentasachride repeating units determines the cross-reactivity of the related O-antigens only to some extent, whereas the terminal residue of the side-branched i.e. α-D-Fuc3N with amido-linked non-carbohydrate substituent, defines the specificity of the O-serotypes. In addition, it seems that the presence of β-D-QuiNAc in the main chain of the A4 and Pt679 O-antigens affects the serological specificity and similarity of these two strains and at the same time determines the minor serological differences between A4 and K928 OPS, where β-D-QuiNAc is replaced by β-D-FucNAc. Therefore, we propose separating the *Aeromonas* sp. PGO1 serogroup into subgroups for strains/O-serotypes that share common structural elements within the branched pentasaccharide repeating unit but differ in non-carbohydrate substituents located at the terminal α-D-Fuc3N. Based on this, the PGO1a subgroup comprises O-serotypes containing the terminal α-D-Fuc3N with 3-hydroxybutanoyl group as the main immunoreactive epitope and is represented by the A4 and K928 strains, and the other PGO1b subgroup, with the terminal α-D-Fuc3NAc, is represented by the Pt679 strain.

Considering the serological and structural heterogeneity of the *Aeromonas* sp. PGO1 serogroup, dominant in Polish aquaculture [34], the proposed division may not be final and requires further studies.

Comprehensive phenotype and genotype studies undertaken to characterize and compare the related O-antigens of *A. hydrophila* Pt679, *A. popoffii* A4, and *A. sobria* K928 classified into the PGO1 serogroup prevailing in Polish aquaculture of carp and rainbow trout seem to be the most appropriate approach. The representatives of the PGO1 serogroup are the first three strains whose O-serotypes have been completely genetically and structurally recognized. The composition of the genetic regions was consistent with the chemical structure of the O-antigens. Moreover, it was revealed that *Aeromonas* strains possessing closely related O-antigens share a high identity level of their OGCs; however, there are some specific structural elements that determine the uniqueness of the individual O-serotypes. The recognition of the O-antigen structure and genetics of the OGC within strains of the same serogroup will contribute to the development of PCR-based molecular biology methods for faster serotyping of *Aeromonas* spp. responsible for severe MAI/MAS infections in aquacultures and improve selection of vaccine candidates for immunoprophylaxis.

Declaration of competing interest

The authors declare that they have no known competing financial interests or personal relationships that could have appeared to influence the work reported in this paper.

Data availability

Data will be made available on request.

Acknowledgments

The authors wish to thank Doctor Paweł Sowiński for recording the NMR spectra (Intercollegiate NMR Laboratory, Department of Chemistry, Technical University of Gdansk, Poland) and MSc Hubert Pietras for his technical support in LPS isolation.

The authors wish to thank Professor Alicja Kozińska for her kind gift of the reference PGO1 antiserum.

Appendix A. Supplementary data

Supplementary data to this article can be found online at https://doi.org/10.1016/j.carres.2023.108896.

References

[1] A. Fernández-Bravo, M.J. Figueras, An update on the genus *Aeromonas*: taxonomy, epidemiology, and pathogenicity, Microorganisms 8 (2020) 129, https://doi.org/10.3390/microorganisms8010129.

[2] A. Kozińska, A. Pękala, Serotyping of *Aeromonas* species isolated from Polish fish farms in relation to species and virulence phenotype of the bacteria, Bull. Vet. Inst. Pulawy 54 (2010) 315–320.

[3] M. Shirajum Monir, S.M. Yusoff, A. Mohamad, M.Y. Ina-Salwany, Vaccination of Tilapia against motile *Aeromonas* septicemia: a review, J. Aquat. Anim. Health 32 (2020) 65–76, https://doi.org/10.1002/aah.10099.

[4] T. Citarasu, K. Alfred Dhas, S. Velmurugan, V. Thanga Viji, T. Kumaran, M. Michael Babu, T. Selvaraj, Isolation of *Aeromonas hydrophila* from infected ornamental fish hatchery during massive disease, outbreak 2 (2011) 37–41.

[5] J. Matys, A. Turska-Szewczuk, A. Sroka-Bartnicka, Role of bacterial secretion systems and effector proteins - insights into *Aeromonas* pathogenicity mechanisms, Acta Biochim. Pol. 67 (2020) 283–293, https://doi.org/10.18388/abp.2020_5410.

[6] C. Whitfield, D.M. Williams, S.D. Kelly, Lipopolysaccharide O-antigens bacterial glycans made to measure, J. Biol. Chem. 295 (2020) 10593–10609, https://doi.org/10.1074/jbc.REV120.009402.

[7] F. Di Lorenzo, C. De Castro, A. Silipo, A. Molinaro, Lipopolysaccharide structures of Gram-negative populations in the gut microbiota and effects on host interactions, FEMS Microbiol. Rev. 43 (2019) 257–272, https://doi.org/10.1093/femsre/fuz002.

[8] L.R. Stromberg, N.W. Hengartner, K.L. Swingle, R.A. Moxley, S.W. Graves, G. A. Montaño, H. Mukundan, Membrane insertion for the detection of lipopolysaccharides: exploring the dynamics of amphiphile-in-lipid assays, PLoS One 11 (2016), e0156295, https://doi.org/10.1371/journal.pone.0156295.

[9] Y. Li, P. Xia, J. Wu, A. Huang, G. Bu, F. Meng, F. Kong, X. Cao, X. Han, G. Yu, X. Pan, S. Yang, X. Zeng, X. Du, The potential sensing molecules and signal cascades for protecting teleost fishes against lipopolysaccharide, Fish Shellfish Immunol. 97 (2020) 235–247, https://doi.org/10.1016/j.fsi.2019.12.050.

[10] B. Liu, A. Furevi, A.V. Perepelov, X. Guo, H. Cao, Q. Wang, P.R. Reeves, Y.A. Knirel, L. Wang, G. Widmalm, Structure and genetics of *Escherichia coli* O antigens, FEMS Microbiol. Rev. 44 (2020) 655–683, https://doi.org/10.1093/femsre/fuz028.

[11] S.T. Islam, J.S. Lam, Synthesis of bacterial polysaccharides via the Wzx/Wzy-dependent pathway, Can. J. Microbiol. 60 (2014) 697–716, https://doi.org/10.1139/cjm-2014-0595.

[12] X. Yu, A. Torzewska, X. Zhang, Z. Yin, D. Drzewiecka, H. Cao, B. Liu, Y.A. Knirel, A. Rozalski, L. Wang, Genetic diversity of the O antigens of *Proteus species* and the development of a suspension array for molecular serotyping, PLoS One 12 (2017), e0183267, https://doi.org/10.1371/journal.pone.0183267.

[13] W.J. Keenleyside, C. Whitfield, A novel pathway for O-polysaccharide biosynthesis in *Salmonella enterica* serovar *borreze*, J. Biol. Chem. 271 (1996) 28581–28592, https://doi.org/10.1074/jbc.271.45.28581.

[14] M. Kurzylewska, K. Dworaczek, A. Turska-Szewczuk, Structure of the lipopolysaccharide O-antigen of *Aeromonas encheleia* strain A4 representing the new PGO1 serogroup of aeromonads prevailing in Polish aquaculture, Carbohydr. Res. 519 (2022), 108602, https://doi.org/10.1016/j.carres.2022.108602.

[15] M. Kurzylewska, A. Bomba, K. Dworaczek, A. Pękala-Safińska, A. Turska-Szewczuk, Structure and gene cluster annotation of the O-antigen of *Aeromonas sobria* strain K928 isolated from common carp and classified into the new *Aeromonas* PGO1 serogroup, Carbohydr. Res. (2023), 108809, https://doi.org/10.1016/j.carres.2023.108809.

[16] R. Sakazaki, T. Shimada, O-serogrouping scheme for mesophilic *Aeromonas* strains, Jpn. J. Med. Sci. Biol. 37 (1984) 247–255, https://doi.org/10.1016/S0923-2508(98)80323-9.

[17] A. Kozińska, Genotypic and serological analysis of domestic mesophilic isolates *Aeromonas* sp. in terms of pathogenicity and the type of disease symptoms caused by them in fish, in: Habilitation Thesis, The National Veterinary Institute—The National Research Institute, Puławy, Poland, 2009.

[18] O. Westphal, K. Jann, Bacterial lipopolysaccharides. Extraction with phenol water and further applications of the procedure, in: R.L. Whistler (Ed.), Methods Carbohydr. Chem., Academic Press, New York, 1965, pp. 83–91.

[19] C.M. Tsai, C.E. Frasch, A sensitive silver stain for detecting lipopolysaccharides in polyacrylamide gels, Anal. Biochem. 119 (1982) 115–119, https://doi.org/10.1016/0003-2697(82)90673-X.

[20] Z. Sidorczyk, K. Zych, F.V. Toukach, N.P. Arbatsky, A. Zablotni, A.S. Shashkov, Y. A. Knirel, Structure of the O-polysaccharide and classification of *Proteus mirabilis* strain G1 in *Proteus* serogroup O3, Eur. J. Biochem. 269 (2002) 1406–1412, https://doi.org/10.1046/j.1432-1033.2002.02782.x.

[21] K. Dworaczek, D. Drzewiecka, A. Pękala-Safińska, A. Turska-Szewczuk, Structural and serological studies of the O6-related antigen of *Aeromonas veronii* bv. *sobria* strain K557 ssolated from *Cyprinus carpio* on a Polish fish farm, which contains l-perosamine (4-amino-4,6-dideoxy-l-mannose), a unique sugar characteristic for *Aeromonas* serogroup O6, Mar. Drugs 17 (2019) 399, https://doi.org/10.3390/md17070399.

[22] D. Drzewiecka, N.P. Arbatsky, A.S. Shashkov, P. Stączek, Y.A. Knirel, Z. Sidorczyk, Structure and serological properties of the O-antigen of two clinical *Proteus mirabilis* strains classified into a new *Proteus* O77 serogroup, FEMS Immunol. Med. Microbiol. 54 (2008) 185–194, https://doi.org/10.1111/j.1574-695X.2008.00462.x.

[23] I. Ciucanu, F. Kerek, A simple and rapid method for the permethylation of carbohydrates, Carbohydr. Res. 131 (1984) 209–217, https://doi.org/10.1016/0008-6215(84)85242-8.

[24] K. Leontein, B. Lindberg, J. Lönngren, Assignment of absolute configuration of sugars by g.l.c. of their acetylated glycosides formed from chiral alcohols, Carbohydr. Res. 62 (1978) 359–362, https://doi.org/10.1016/S0008-6215(00)80882-4.

[25] S. Chen, Y. Zhou, Y. Chen, J. Gu, Fastp: an ultra-fast all-in-one FASTQ preprocessor, Bioinformatics 34 (2018) 884–890, https://doi.org/10.1093/bioinformatics/bty560.

[26] S. Andrews, FastQC: A Quality Control Tool for High Throughput Sequence Data, 2010. https://www.bioinformatics.babraham.ac.uk/projects/fastqc/. (Accessed 9 January 2023).

[27] A. Bankevich, S. Nurk, D. Antipov, A.A. Gurevich, M. Dvorkin, A.S. Kulikov, V. M. Lesin, S.I. Nikolenko, S. Pham, A.D. Prjibelski, A.V. Pyshkin, A.V. Sirotkin, N. Vyahhi, G. Tesler, M.A. Alekseyev, P.A. Pevzner, SPAdes: a new genome assembly algorithm and its applications to single-cell sequencing, J. Comput. Biol. 19 (2012) 455–477, https://doi.org/10.1089/cmb.2012.0021.

[28] A. Mikheenko, A. Prjibelski, V. Saveliev, D. Antipov, A. Gurevich, Versatile genome assembly evaluation with QUAST-LG, Bioinformatics 34 (2018) 142–150, https://doi.org/10.1093/bioinformatics/bty266.

[29] T. Seemann, Prokka: rapid prokaryotic genome annotation, Bioinformatics 30 (2014) 2068–2069, https://doi.org/10.1093/bioinformatics/btu153.

[30] H. Cao, M. Wang, Q. Wang, T. Xu, Y. Du, H. Li, C. Qian, Z. Yin, L. Wang, Y. Wei, P. Wu, X. Guo, B. Yang, B. Liu, Identifying genetic diversity of O antigens in *Aeromonas hydrophila* for molecular serotype detection, PLoS One 13 (2018), e0203445, https://doi.org/10.1371/journal.pone.0203445.

[31] C.L.M. Gilchrist, Y.H. Chooi, Clinker & clustermap.js: automatic generation of gene cluster comparison figures, Bioinformatics 37 (2021) 2473–2475, https://doi.org/10.1093/bioinformatics/btab007.

[32] A.J. Martinez-Murcia, A. Monera, M.J. Saavedra, R. Oncina, M. Lopez-Alvarez, E. Lara, M.J. Figueras, Multilocus phylogenetic analysis of the genus *Aeromonas*, Syst. Appl. Microbiol. 34 (2011) 189–199, https://doi.org/10.1016/j.syapm.2010.11.014.

[33] K. Katoh, D.M. Standley, MAFFT multiple sequence alignment software version 7: improvements in performance and usability, Mol. Biol. Evol. 30 (2013) 772–780, https://doi.org/10.1093/molbev/mst010.

[34] K. Dworaczek, M. Kurzylewska, M. Laban, D. Drzewiecka, A. Pękala-Safińska, A. Turska-Szewczuk, Structural studies of the lipopolysaccharide of *Aeromonas veronii* bv. sobria strain K133 which represents new provisional serogroup PGO1 prevailing among mesophilic Aeromonads on polish fish farms, Int. J. Mol. Sci. 22 (2021) 4272, https://doi.org/10.3390/ijms22084272.

[35] K. Bock, C. Pedersen, Carbon-13 nuclear magnetic resonance spectroscopy of monosaccharides, Adv. Carbohydr. Chem. Biochem. 41 (1983) 27–66, https://doi.org/10.1016/S0065-2318(08)60055-4.

[36] A. Turska-Szewczuk, A. Kozińska, R. Russa, O. Holst, The structure of the O-specific polysaccharide from the lipopolysaccharide of *Aeromonas bestiarum* strain 207, Carbohydr. Res. 345 (2010) 680–684, https://doi.org/10.1016/j.carres.2009.12.030.

[37] B. Yang, S.N. Senchenkova, O.I. Naumenko, A.S. Shashkov, B. Liu, A.V. Perepelov, Y.A. Knirel, Structural and genetic relatedness of the O-antigens of *Escherichia coli* O50 and O2, Carbohydr. Res. 464 (2018) 8–11, https://doi.org/10.1016/j.carres.2018.05.001.

[38] P.-E. Jansson, H. Lennholm, B. Lindberg, U. Lindquist, Structural Studies of the O-specific Side-Chains of the *Escherichia coli* O2 Lipopolysaccharide, vol. 161, 1987, pp. 273–279, https://doi.org/10.1016/S0008-6215(00)90084-3.

[39] P.-E. Jansson, L. Kenne, G. Widmalm, Computer-assisted structural analysis of polysaccharides with an extended version of casper using 1H- and 13C-n.m.r. data, Carbohydr. Res. 188 (1989) 169–191, https://doi.org/10.1016/0008-6215(89)84069-8.

[40] G.M. Lipkind, A.S. Shashkov, Y.A. Knirel, E.V. Vinogradov, N.K. Kochetkov, A computer-assisted structural analysis of regular polysaccharides on the basis of 13C-N.M.R. data, Carbohydr. Res. 175 (1988) 59–75, https://doi.org/10.1016/S0008-6215(01)00214-2.

[41] A. Molinaro, A. Silipo, R. Lanzetta, M.-A. Newman, J.M. Dow, M. Parrilli, Structural elucidation of the O-chain of the lipopolysaccharide from *Xanthomonas campestris* strain 8004, Carbohydr. Res. 338 (2003) 277–281, https://doi.org/10.1016/S0008-6215(02)00433-0.

[42] A.S. Shashkov, G.M. Lipkind, Y.A. Knirel, N.K. Kochetkov, Stereochemical factors determining the effects of glycosylation on the 13C chemical shifts in carbohydrates, Magn. Reson. Chem. 26 (1988) 735–747, https://doi.org/10.1002/mrc.1260260904.

[43] O.V. Sizova, A.S. Shashkov, A.N. Kondakova, Y.A. Knirel, R.Z. Shaikhutdinova, S. A. Ivanov, A.A. Kislichkina, L.A. Kadnikova, A.G. Bogun, S.V. Dentovskaya, Full structure and insight into the gene cluster of the O-specific polysaccharide of *Yersinia intermedia* H9-36/83 (O:17), Carbohydr. Res. 460 (2018) 51–56, https://doi.org/10.1016/j.carres.2018.02.014.

[44] A. Pfoestl, A. Hofinger, P. Kosma, P. Messner, Biosynthesis of dTDP-3-acetamido-3,6-dideoxy-α-D-galactose in *Aneurinibacillus thermoaerophilus* L420-91T, J. Biol. Chem. 278 (2003) 26410–26417, https://doi.org/10.1074/jbc.M300858200.

[45] B. Liu, A.V. Perepelov, M.V. Svensson, S.D. Shevelev, D. Guo, S.N. Senchenkova, A. S. Shashkov, A. Weintraub, L. Feng, G. Widmalm, Y.A. Knirel, L. Wang, Genetic and structural relationships of *Salmonella* O55 and *Escherichia coli* O103 O-antigens and identification of a 3-hydroxybutanoyltransferase gene involved in the synthesis of a Fuc3N derivative, Glycobiology 20 (2010) 679–688, https://doi.org/10.1093/glycob/cwq015.

[46] J.D. King, D. Kocíncová, E.L. Westman, J.S. Lam, Lipopolysaccharide biosynthesis in Pseudomonas aeruginosa, Innate Immun. 15 (2009) 261–312, https://doi.org/10.1177/1753425909106436.

[47] G. Samuel, P. Reeves, Biosynthesis of O-antigens: genes and pathways involved in nucleotide sugar precursor synthesis and O-antigen assembly, Carbohydr. Res. 338 (2003) 2503–2519, https://doi.org/10.1016/j.carres.2003.07.009.

[48] K.H.M. Jonsson, A. Weintraub, G. Widmalm, Structural determination of the O-antigenic polysaccharide from *Escherichia coli* O74, Carbohydr. Res. 344 (2009) 1592–1595, https://doi.org/10.1016/j.carres.2009.03.023.

[49] A.V. Perepelov, A.V. Filatov, M. Wang, A.S. Shashkov, L. Wang, Y.A. Knirel, Structure and gene cluster of the O-antigen of *Enterobacter cloacae* G3421, Carbohydr. Res. 427 (2016) 55–59, https://doi.org/10.1016/j.carres.2016.03.008.

[50] Y. Bi, E. Mann, C. Whitfield, J. Zimmer, Architecture of a channel-forming O-antigen polysaccharide ABC transporter, Nature 176 (2018) 139–148, https://doi.org/10.1038/nature25190.

[51] B. Liu, Y.A. Knirel, L. Feng, A.V. Perepelov, S.N. Senchenkova, P.R. Reeves, L. Wang, Structural diversity in *Salmonella* O antigens and its genetic basis, FEMS Microbiol. Rev. 38 (2013) 56–89, https://doi.org/10.1111/1574-6976.12034.

[52] B. Liu, A.V. Perepelov, M.V. Svensson, S.D. Shevelev, D. Guo, S.N. Senchenkova, A. S. Shashkov, A. Weintraub, L. Feng, G. Widmalm, Y.A. Knirel, L. Wang, Genetic and structural relationships of *Salmonella* O55 and *Escherichia coli* O103 O-antigens and identification of a 3-hydroxybutanoyltransferase gene involved in the synthesis of a Fuc3N derivative, Glycobiology 20 (2010) 679–688, https://doi.org/10.1093/glycob/cwq015.

[53] P.M. Fratamico, C. DebRoy, T.P. Strobaugh, C.Y. Chen, DNA sequence of the *Escherichia coli* O103 O antigen gene cluster and detection of enterohemorrhagic *E. coli* O103 by PCR amplification of the wzx and wzy genes, Can. J. Microbiol. 51 (2005) 515–522, https://doi.org/10.1139/w05-049.

[54] C.M. Thurlow, M.J. Hossain, D. Sun, P. Barger, L. Foshee, B.H. Beck, J.C. Newton, J.S. Terhune, M.A. Saper, M.R. Liles, The gfc operon is involved in the formation of the O antigen capsule in *Aeromonas hydrophila* and contributes to virulence in channel catfish, Aquaculture 512 (2019), 734334, https://doi.org/10.1016/j.aquaculture.2019.734334.